Organic & Biomolecular Chemistry

ROYAL SOCIETY OF CHEMISTRY

PAPER

View Article Online
View Journal | View Issue

Cite this: *Org. Biomol. Chem.*, 2023, **21**, 7136

Diastereoisomeric enrichment of 1,4-enediols and H_2-splitting inhibition on Pd-supported catalysts†

Jordi Ballesteros-Soberanas, Marta Mon and Antonio Leyva-Pérez *

Received 27th June 2023,
Accepted 16th August 2023

DOI: 10.1039/d3ob01025b

rsc.li/obc

Pd-supported catalysts are fundamental tools in organic reactions involving H_2 splitting. Here we show that 1,4-enediols enriched in one diastereoisomer are produced from the classical Pd-catalyzed semi-hydrogenation reaction with H_2, starting from the corresponding, widely available 1,4-diacetylenic diols. The semi-hydrogenation reaction proceeds concomitantly with the desymmetrization of the *meso*/racemic form of the enediol. We also show that these products, if added in advance to H_2, completely inactivate the Pd catalyst (only when added before H_2). These results provide a simple way not only to produce 1,4-enediols enriched in one diastereoisomer by a classical catalytic method but also to stop H_2 dissociation on Pd nanoparticles.

1 Introduction

Pd supported catalysts such as Pd on carbon (Pd/C) and the Lindlar catalyst (Pd–Pb–$CaCO_3$) are recurrently used in organic synthesis to catalyze the hydrogenation of reducible functional groups.[1] The challenge usually consists in stopping the reaction at the desired functionality, since the Pd catalyst splits and transfers H_2 so efficiently that over-hydrogenation reactions occur (alkyne → alkene → alkane, nitro → oxime → amine,...).[2,3] Thus, the strong ability of Pd catalysts to activate H_2 is largely presupposed by the scientific community.

We report here that the semi-hydrogenation reaction of 1,4-acetylene diols **1** on simple Pd catalysts proceeds in a diastereoselective way to give 1,4-enediols **2** (*meso* form) preferentially and **3** (racemic form) and, furthermore, that the 1,4-enediol products **2 and 3** completely poison the Pd catalyst inhibiting further splitting of H_2, as shown in Fig. 1. The drastic inhibition of H_2 reactivity on Pd-supported catalysts by complex molecules is extremely rare and opens new ways to manage H_2 gas in the presence of Pd catalysts. This effect may also explain the spontaneous diastereoisomeric enrichment found during the semi-hydrogenation reaction of these substrates.

1,4-Enediols constitute a family of gemini-type compounds with wide use in industry as emulsifiers, fragrances and drugs, among other applications.[4–6] Their synthesis relies on two methodologies: the classical *cis*-selective Pd-catalyzed semi-hydrogenation of 1,4-acetylene diols, studied in this work in depth for the first time as far as we know, and the *trans*-selective semi-hydrogenation of the same alkynes with stoichiometric $LiAlH_4$.[7,8]

We could not find specific studies for the semi-hydrogenation reaction of 1,4-acetylene diols in the literature, except for a seminal study published 70 years ago,[9] which focused on the competing full hydrogenation and hydrogenolysis reactions of **2–4**, to give products **5** and **6**. However, synthetic researchers recurrently employ the stoichiometric method with $LiAlH_4$ [7,8] and also the classical catalytic hydrogenation to prepare a variety of 1,4-enediols, from industrial compounds[10] to more elaborate academic molecules.[11–17] However, a significant diastereo enrichment (>1.5 : 1) of the *meso* form is not reported yet, to our knowledge.[9,11]

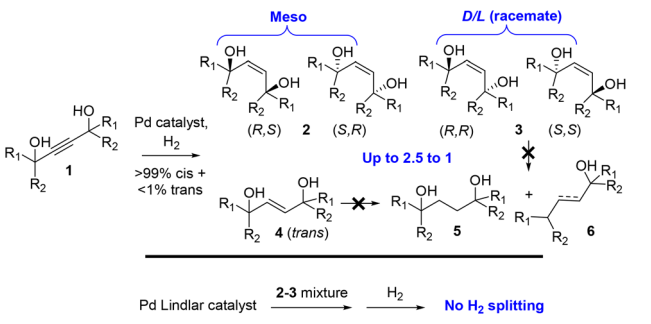

Fig. 1 The spontaneous diastereo-enriched formation of alkenediols **2** during the semi-hydrogenation reaction of alkynes **1** catalyzed by classical Pd catalysts (*i.e.* Lindlar catalyst) and the complete inhibition of H_2 splitting when the Pd catalyst is previously impregnated with **2 and 3**.

Instituto de Tecnología Química (UPV-CSIC), Universidad Politècnica de València-Consejo Superior de Investigaciones Científicas, Avda. de los Naranjos s/n, 46022 Valencia, Spain. E-mail: anleyva@itq.upv.es

†Electronic supplementary information (ESI) available: Experimental details, Fig. S1–S12, Tables S1–S5, compound characterization and NMR copies. See DOI: https://doi.org/10.1039/d3ob01025b

2 Results and discussion

2.1 Pd-catalyzed semi-hydrogenation reaction of 1,4-diacetylenic diols

2.1.1 Catalyst screening. Table 1 shows the catalytic results for the semi-hydrogenation reaction of 2,4,7,9-tetramethyl-5-decyn-4,7-diol **1a** (TMDD) with different metal catalysts (see Tables S1 and S2 in the ESI† for further details). TMDD is a widely used industrial vehicle agent[18–20] and the corresponding 1,4-enediol products **2a–4a** find application as phase transfer agents.[20] The metal catalysts tested here include typical Pd catalysts for selective alkyne semi-hydrogenation reactions, *i.e.* the Lindlar catalyst,[21] colloidal Pd nanoparticles stabilized with hexadecyl(2-hydroxyethyl)dimethyl ammonium dihydrogenphosphate (HHDMA) ligands developed by BASF (c-Pd/TiS, NanoSelect™)[22,23] and a soluble catalyst based on $CaCO_3$ clusters, recently developed by our group[24,25] to avoid Pb in the catalyst,[26,27] and also benchmark hydrogenation catalysts such as Pd/C, Pt/C and Ni RANEY®.

The catalytic results show that small amounts of the different Pd catalysts (0.003–0.15 mol%, Table 1, entries 1–3) give on average an ~1.5 to 1 ratio of the *meso* form **2a** with respect to the D/L form **3a**, with low formation of *trans* **4a** or alkane products **5a–6a**. However, according to the experiments performed with the Lindlar catalyst (entry 1), the diastereoisomeric ratio can be increased by changing the reaction conditions (pressure, reaction time, and solvent): the diastereoisomeric *meso* : D/L ratio (**2a**/**3a**) improves to 2 when increasing H_2 pressure and concentration and to 2.5 when changing the solvent from ethanol to toluene (see also Table S1†). The quantification of the different regioisomers is based on the assignation of the corresponding signals by combined gas-chromatography-mass spectrometry (GC-MS, Fig. S1†), ^{1}H, ^{13}C and distortionless enhancement by polarization transfer (DEPT) nuclear magnetic resonance (NMR, Fig. S2†), including 2D-nuclear Overhauser enhancement spectroscopy (NOESY, Fig. S3†), the independent synthesis of the *trans* product **4a** by the $LiAlH_4$ method, and comparison with literature data.[9,14] The commercial non-selective catalysts exhibit prominent alkane formation along with undesired hydrogenolytic reactions (entries 4–6 in Table 1, see also Table S2†). The significant diastereo enrichment found here with Pd catalysts (up to 2.5 : 1) is much higher than any results previously reported.[9,11]

2.1.2 Substrate scope. We then synthesized different symmetric and asymmetric 1,4-acetylene diols **1b–h** (see the ESI†) and tested them in the semi-hydrogenation reaction under the optimized reaction conditions, as shown in Fig. 2. In all cases, milder reaction conditions than for **1a** were required to avoid undesired side-reactions (see Table S3†). The enrichment of the *meso* diastereoisomer in the mixture is observed for half of the alkynes tested, which indicates that this effect is reasonably general during the semi-hydrogenation reaction of 1,4-acetylene diols.[28] We tried to separate the enediol mixtures by preparative thin-layer chromatography (TLC). Unfortunately, even after running the TLC at very slow velocity, the product mixture could not be separated. We also tried to separate the mixture after derivatization to either ethers (*i.e.* pyranes), esters or siloxy compounds; however, the reactions did not proceed quantitatively and the product mixtures could not be separated either.

2.1.3 Diastereoisomeric enrichment mechanism. The diastereoisomeric enrichment might proceed from the epimerization of the C–OH bond, either in alkyne **1** or alkenes **2**/**3**.[29–33] This hypothesis is supported by solvent screening (Table S2†), which reveals dependency of the diastereoisomeric ratio on the polarity of the solvent, maximized for intermediate polarities (such as toluene), suggesting that an SN_1 process could be operating here. To test this, the starting 1,4-acetylene diol **1a** was placed in the presence of the Lindlar catalyst (0.15 mol%) and $H_2O(^{18}O)$ (15 equivalents), and the reaction was monitored by GC-MS. The results (Table S4 and Fig. S4†) show that the quaternary C–OH bond in **1a** incorporates 48%

Table 1 Catalyst screening for the semi-hydrogenation reaction of TMDD **1a**. The amount of metal catalyst employed is the minimum amount that was found to achieve full conversion under the indicated reaction conditions. The mass balance is completed with dihydroxylation products. The *trans* enediol **4a** was typically <1%

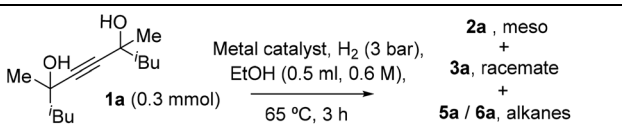

Entry	Catalyst (metal mol%)	**2a** (%)	**3a** (%)	**5a**/**6a** (%)	**2a**/**3a**
1	Lindlar (0.15)	53 (58)[a] (64)[b]	34 (29)[a] (25)[b]	13 (0)[a] (0)[b]	1.55 (2.00)[a] (2.50)[b]
2	c-Pd/TiS (0.015)	59	34	7	1.44
3	Pd-$(CaCO_3)_n$ (0.003)	53	42	5	1.26
4	Pd/C (0.04)	15	9	76	1.60
5	Pt/C (0.018)	28	20	52	1.37
6	Ni-RANEY® (25)	25	21	54	1.15

[a] 10 bar H_2, 12 h reaction time, 1 M EtOH. [b] 1 M toluene as a solvent, 12 h reaction time.

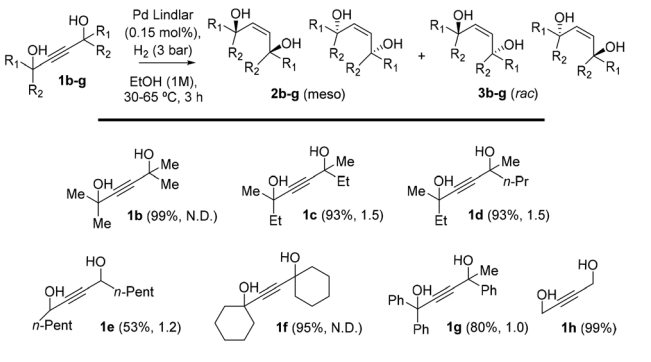

Fig. 2 Catalytic results for different 1,4-acetylene diols **1b–h** during the semi-hydrogenation reaction under the indicated reaction conditions (see also Table S3†). Within parentheses are shown the reaction yield and diastereoisomeric ratio. N.D.: isomers not distinguishable by GC and NMR.

of ^{18}O (**1a**-^{18}**O**). This incorporation does not occur without the Pd catalyst, which suggests that the diastereoisomeric enrichment of the *meso* form may occur by epimerization of the C–OH bond of **1** catalyzed by Pd, prior to hydrogenation. Fig. 3 depicts this process.

To check that the epimerization reaction occurs in alkyne **1a** without requiring the participation of H_2, the semi-hydrogenation products **2a**/**3a** were also placed in the presence of the Lindlar catalyst and $H_2O(^{18}O)$ (as above), and the results (see again Table S4 and Fig. S4†) show that the quaternary C–OH bonds in **2a**/**3a** incorporate just 6% of ^{18}O atoms. This is congruent with the higher stability of the propargyl cation. Molecular mechanics calculations (MM2) show that the stabilization energy for the propargyl cation is just 12 kcal mol^{-1}, and that the minimum stabilization energy for the *meso* form of **1a** is slightly higher than that of the *rac* form, although product *meso* **2a** is slightly less stable than *rac* **3a** (see Fig. 3). These results support the fact that the epimerization occurs on the alkyne products rather than on the alkene products. The incorporation of ^{18}O atoms under H_2 could not be conveniently assessed by the coincidence of masses in the hydrogenated products and the isotopically-labelled products.

It is true that the reaction does not canonically produce water, but water is not strictly necessary for the epimerization, since the simple formation of the highly stabilized propargyl cation of alkyne **1a** generated a nucleophilic OH^- to carry out the epimerization reaction (see Fig. 3). Indeed, H_2O must be present in traces during the reaction, supplied by the reactants, solvent or catalyst support. Even any trace of air in the reaction system will produce water after reaction with H_2. Thus, some water molecules must be present during the reaction anyway.

This mechanism is in line with the substrate scope results shown in Fig. 2. There, it can be seen that tertiary alcohols that are able to stabilize better the carbocation in the tertiary carbon atom, after H_2O release, are indeed the higher yielding substrates (*i.e.* products **1a–d** and **1f**), while secondary alcohols and tertiary alcohols that are not so prone to stabilize the carbocation only gave moderate results (products **1e** and **1g**, respectively).

2.2 Inhibition of H_2 splitting on the Pd catalyst

2.2.1 Gemini alkenediols as powerful Pd poisons. A typical experiment to assess alkene selectivity during the semi-hydrogenation reaction consists in carrying out the catalytic process with the alkene product as the starting material. Thus, we placed the alkene mixture **2a**/**3a** in the presence of the Lindlar catalyst under the reaction conditions indicated in Table 1 and started the reaction. Perhaps not surprisingly, the reaction did not proceed at all, which may indicate that alkenes **2a**/**3a** are very unreactive towards the hydrogenation reaction (Fig. 1 bottom).[34,35] However, the hydrogenation reaction of **1a** proceeded with <10% conversion when **1a** was mixed with **2a**/**3a** from the beginning (60 : 40, Fig. S5†), which is extremely rare considering that the reaction proceeds from **1a** to **2a**/**3a**. Fig. 4 shows that this lack of catalytic activity of the Lindlar catalyst when **1a** and **2a**/**3a** are present from the beginning of the reaction also occurs when the semi-hydrogenation reaction is halted by simply releasing the H_2 atmosphere and letting air seep into the reaction mixture, at ~50–70% conversion (>99% selectivity to **2a**/**3a**). Notice that pressurizing back with H_2 does not re-start the reaction and, indeed, the inhibition persists if the Lindlar catalyst is filtered off and washed with ethanol (Fig. S5†). The inhibition effect also occurs in toluene (Fig. S6 and S7†), and thus it seems to be independent of the solvent used, and the *trans* enediol **4a** also inhibits the catalyst. In contrast, the reaction proceeds to completion if H_2 is present from the beginning. Moreover, if the reaction time is extended further and more Pd catalyst is added in order to achieve an over-hydrogenation reaction and get the alkane product **5a**/**6a**, the solid then retains some of the catalytic activity after recovery (Fig. S5†). These combined results suggest that the enediol products **2a–4a** poison the Lindlar catalyst in the hydrogenation reaction, provided that H_2 is not introduced before, since in that case the semi-hydrogenation reaction proceeds normally.

2.2.2 Other Pd-catalyzed hydrogenation reactions. In order to check if 1,4-enediols are general inhibitors of Pd-supported catalysts, provided that they are added before H_2, the hydrogenation of nitrobenzene **7** or acetophenone **9** was carried out in the presence of the Lindlar catalyst and also a commercial sample of Pd/C, with or without impregnation with **2a**/**3a**. Fig. 5 shows that the hydrogenation reaction is hampered when the 1,4-enediol is added in the starting mixture, for both Pd-supported solid catalysts, giving products aniline **8** and phenylethanol-ethylbenzene **10–11**, respectively, in low yields compared to the mixture without enediols. The reduction of the nitro group does not stop at the nitroso group or the oxime

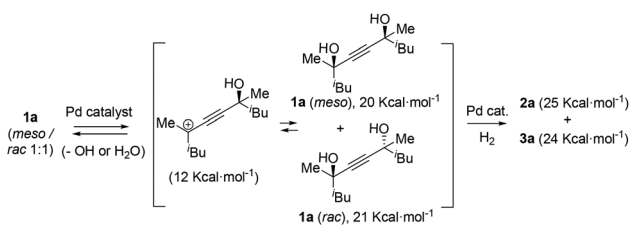

Fig. 3 The proposed mechanism for the diastereo-differentiation found in products **2a**/**3a**. Energy values correspond to the minimum stabilization energy found for the corresponding molecules and intermediates according to molecular mechanics calculations in a vacuum (MM2).

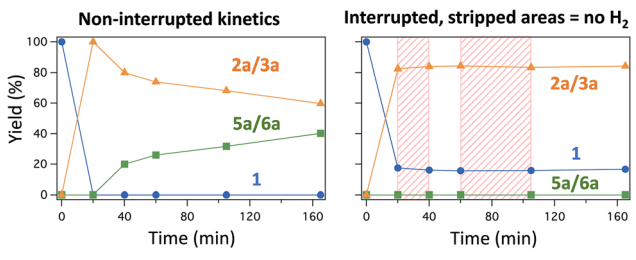

Fig. 4 Kinetics for the semi-hydrogenation reaction of TMDD **1** catalyzed by the Lindlar catalyst (0.5 mol%) at 10 bar H_2, 1 M EtOH and 65 °C, either continuous (left) or interrupted after H_2 release and re-filling (right).

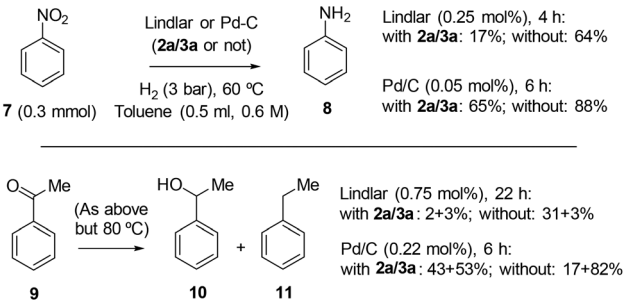

Fig. 5 Results for the hydrogenation reaction of nitrobenzene **7** (top) and acetophenone **9** (bottom) in the presence of different Pd-supported catalysts (Lindlar or Pd/C) with or without impregnation with enediols **2a**/**3a**, at 3 bar H_2 and 0.6 M toluene and under the indicated reaction conditions, optimized for each catalyst and reaction. Selectivity towards the indicated products is >95% in all cases, and nitroso or oxime intermediates were not found for **7**. Notice that for **9**, the fully hydrogenated product **11** is the major product without **2a**/**3a**.

group and directly goes to the amine group, even at intermediate conversions. Phenylacetylene was also tested as a reactant under the optimized reaction conditions with or without the poisoning agents **2a**/**3a** (Table S5†), and the results show how the hydrogenation reaction is hampered in the presence of the alkenediols. These results suggest that the addition of **2a**/**3a** can control the selectivity of different hydrogenation reactions.

2.2.3 Inhibition mechanism exerted by the gemini alkenediols. Fig. 6 shows a H_2–D_2 isotopic exchange experiment on the Lindlar catalyst, in the presence and absence of **2a**/**3a**. The isotopic exchange yield drops from 54.3% to 1.9% due to the presence of **2a**/**3a**, clearly indicating that the formation of H–D does not occur if the solid catalyst is impregnated with **2a**/**3a**. The same phenomenon is observed on the Pd/C surface (Fig. S8†), and the Raman spectrum of Pd/C confirms the inhibition of H_2 splitting after addition of **2a**/**3a** (Fig. S9†). Unfortunately, the corresponding Raman spectrum for the Lindlar catalyst could not be obtained, probably due to a low Pd–H signal strength. These results strongly indicate that enediols **2a**/**3a** are a new class of Lewis bases for Pd nanoparticles, able to completely inhibit the dissociation of H_2 on the surface, which should enable the use of these Pd-based materials in the presence of a H_2 atmosphere without generating hydrogen reactive species.[36–38]

Fourier-transform infrared (FT-IR) spectroscopy supports the strong binding of the diol to the support (Fig. S10†). It can be seen that the original signal at 1441 cm^{-1}, corresponding to the carbonate groups of the Lindlar catalyst, decreases in intensity after adding the 1,4 enediols **2a**/**3a**, with the appearance of a new band at 1404 cm^{-1}. This new band does not correspond to free **2a**/**3a**, as indicated by the relative intensity of the main **2a**/**3a** signals (*i.e.* 2951 *vs.* 1364 cm^{-1}). A fast evaluation of the adsorption mode of alkyne **1a** and alkene **2a** on the surface of different Pd crystalline slabs [(100), (110) and (111)] was carried out with a graph neural network called GAME-Net.[39] The results (Fig. S11†) show that the adsorption process is exothermic in all cases and that the adsorption

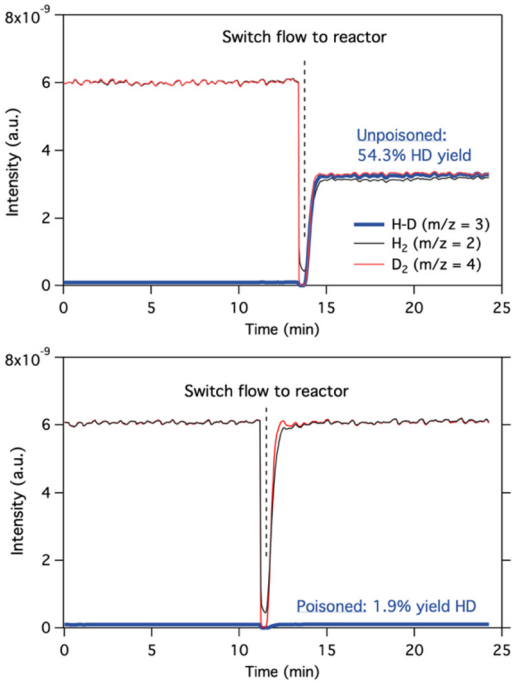

Fig. 6 H_2–D_2 isotopic exchange experiments, at 30 °C, for the fresh Lindlar catalyst (top) and poisoned Lindlar catalyst, with the **2a** + **3a** mixture (bottom).

energy for the alkenes is systematically higher than for the alkyne, >25 kcal mol^{-1} in the case of the more common Pd(111) surface. By modelling the latter (Fig. S12†), it can be seen how alkenes **2a**/**4a** are disposed parallelly to the Pd(111) surface, regardless of the *cis*/*trans* configuration, with the alkene and alcohol groups pointed towards the Pd atoms. These results explain that both **2a** and **4a** poison the Pd surface. The simplest gemini alkynediol 2-butyn-1,4-diol **1h** also shows similar energetic values on Pd surfaces (Fig. S11†). The above results, together, confirm the strong binding of 1,4-enediols to Pd-supported catalysts, inhibiting the H_2 activation, which could also have application in the synthesis of ligand (1,4-enediols)-modified Pd nanoparticles for a variety of applications.

3 Conclusions

We have shown here that the semi-hydrogenation reaction of 1,4-diacetylenic diols catalyzed by different supported Pd catalysts preferentially gives the *meso* form of the enediol, probably by a selective C–OH bond epimerization process, also catalyzed by Pd. The resulting 1,4-enediol products inhibit the dissociation of H_2 on the Pd-supported catalysts if added in the beginning of the hydrogenation reaction, when H_2 is not present yet in the reaction mixture, not only for alkynes but also for nitro and ketone groups. The adsorption mode and strength of 1,4-enediols seem to be the key factors here. These results are of interest to design hydrogenation reactions with classical Pd catalysts.

Author contributions

J. B.-S. performed most of the experimental work and analysis, M. M. studied the scope of functional groups and catalysts, and A. L.-P. supervised the project and wrote the manuscript.

Conflicts of interest

Two patents covering some of these results have been filed: PCT/ES2022/070672 (co-authored by J. B.-S. and A. L.-P.) and P202330474 (co-authored by J. B.-S., M.-M. and A. L.-P.).

Acknowledgements

Financial support by the projects PID2020-115100GB-I00 (funded by Spanish MCIINN, MCIN/AEI/10.13039/501100011033MICIIN), Severo Ochoa Centre of Excellence Program (CEX2021-001230-S) and "La Caixa" Foundation grant (ID 100010434, code LCF/BQ/DI19/11730029) is acknowledged. M. M. thanks MICIIN for support from a contract under the Juan de la Cierva program (FJC2019-040523-I).

References

1 A. O. King, R. D. Larsen and E. Negishi, *Handbook of Organopalladium Chemistry for Organic Synthesis*, Wiley, 2002, pp. 2719–2752.
2 B. Bridier, N. López and J. Pérez-Ramírez, *Dalton Trans.*, 2010, **39**, 8363–8376.
3 A. M. Whittaker and G. Lalic, *Org. Lett.*, 2013, **15**, 1112–1115.
4 C. S. Poss and S. L. Schreiber, *Acc. Chem. Res.*, 1994, **27**, 9–17.
5 M. Hans, M. Charpentier, V. Huch, J. Jauch, T. Bruhn, G. Bringmann and D. Quandt, *J. Nat. Prod.*, 2015, **78**, 2381–2389.
6 F. M. Menger, J. S. Keiper and V. Azov, *Langmuir*, 2000, **16**, 2062–2067.
7 R. K. Hill, S. L. Pendalwar, K. Kielbasinski, M. F. Baevsky and P. N. Nugara, *Synth. Commun.*, 1990, **20**, 1877–1884.
8 L. Grigorjeva, A. Kinens and A. Jirgensons, *J. Org. Chem.*, 2015, **80**, 920–927.
9 R. J. Tedeschi, *J. Org. Chem.*, 1962, **27**, 2398–2402.
10 Y. Qiu, X. Gao, J. Kass, H. W. Cao, X. Li, X. Peng, B. Suh and Y. S. Or, US20190060258A1, 2018.
11 D. Finnegan, B. A. Seigal and M. L. Snapper, *Org. Lett.*, 2006, **8**, 2603–2606.
12 H. Mouhib, W. Stahl, M. Lüthy, M. Büchel and P. Kraft, *Angew. Chem., Int. Ed.*, 2011, **50**, 5576–5580.
13 K. B. Bazhykova, *Russ. J. Org. Chem.*, 2021, **57**, 203–211.
14 X. Ariza, N. Fernández, J. Garcia, M. López, L. Montserrat and J. Ortiz, *Synthesis*, 2004, 128–134.
15 M. J. Burk, J. E. Feaster and R. L. Harlow, *Tetrahedron: Asymmetry*, 1991, **2**, 569–592.
16 J. Bach, R. Berenguer, J. Garcia, T. Loscertales, J. Manzanal and J. Vilarrasa, *Tetrahedron Lett.*, 1997, **38**, 1091–1094.
17 M. Amador, X. Ariza and J. Garcia, *Heterocycles*, 2006, **67**, 705–720.
18 A. A. Guedez, S. Frömmel, P. Diehl and W. Püttmann, *Environ. Sci. Pollut. Res.*, 2010, **17**, 321–330.
19 K. Vincze, M. Gehring and T. Braunbeck, *Environ. Sci. Pollut. Res.*, 2014, **21**, 8233–8241.
20 E. Minnich, EP0940169A1, 1999.
21 G. Vilé, N. Almora-Barrios, S. Mitchell, N. López and J. Pérez-Ramírez, *Chem. – Eur. J.*, 2014, **20**, 5926–5937.
22 P. T. Witte, P. H. Berben, S. Boland and J. G. Donkervoort, *Top. Catal.*, 2012, **55**, 505–511.
23 J. A. Delgado, O. Benkirane, C. Claver, D. Curulla-Ferré and C. Godard, *Dalton Trans.*, 2017, **46**, 12381–12403.
24 J. Ballesteros-Soberanas, J. C. Hernández-Garrido, J. P. Cerón-Carrasco and A. Leyva-Pérez, *J. Catal.*, 2022, **408**, 43–55.
25 J. Ballesteros-Soberanas, J. A. Carrasco and A. Leyva-Pérez, *J. Org. Chem.*, 2023, **88**, 18–26.
26 M. Tejeda-Serrano, M. Mon, B. Ross, F. Gonell, J. Ferrando-Soria, A. Corma, A. Leyva-Pérez, D. Armentano and E. Pardo, *J. Am. Chem. Soc.*, 2018, **140**, 8827–8832.
27 P. McNeice, M. A. Müller, J. Medlock, W. Bonrath, N. Rockstroh, S. Bartling, H. Lund, K. Junge and M. Beller, *ACS Sustainable Chem. Eng.*, 2022, **10**, 9787–9797.
28 S. Mao, B. Zhao, Z. Wang, Y. Gong, G. Lü, X. Ma, L. Yu and Y. Wang, *Green Chem.*, 2019, **21**, 4143–4151.
29 H. Fernández-Pérez, P. Etayo, J. R. Lao, J. L. Núñez-Rico and A. Vidal-Ferran, *Chem. Commun.*, 2013, **49**, 10666–10675.
30 W. Hong, W. A. Swann, V. Yadav and C. W. Li, *ACS Catal.*, 2022, **12**, 7643–7654.
31 H. J. Hu, Q. Q. Wang, D. X. Wang and Y. F. Ao, *Adv. Synth. Catal.*, 2021, **363**, 4538–4543.
32 D. E. Ward, Y. Liu and D. How, *J. Am. Chem. Soc.*, 1996, **118**, 3025–3026.
33 X. Jia, J. Ma, F. Xia, Y. Xu, J. Gao and J. Xu, *Nat. Commun.*, 2018, **9**, 1–7.
34 T. R. Hoye and J. C. Suhadolnik, *J. Am. Chem. Soc.*, 1985, **107**, 5312–5313.
35 H. Wu, Q. Wang and J. Zhu, *Angew. Chem., Int. Ed.*, 2016, **55**, 15411–15414.
36 P. W. Albers, K. Möbus, C. D. Frost and S. F. Parker, *J. Phys. Chem. C*, 2011, **115**, 24485–24493.
37 M. Armbrüster, M. Behrens, F. Cinquini, K. Föttinger, Y. Grin, A. Haghofer, B. Klötzer, A. Knop-Gericke, H. Lorenz, A. Ota, S. Penner, J. Prinz, C. Rameshan, Z. Révay, D. Rosenthal, G. Rupprechter, P. Sautet, R. Schlögl, L. Shao, L. Szentmiklósi, D. Teschner, D. Torres, R. Wagner, R. Widmer and G. Wowsnick, *ChemCatChem*, 2012, **4**, 1048–1063.
38 M. García-Mota, B. Bridier, J. Pérez-Ramírez and N. López, *J. Catal.*, 2010, **273**, 92–102.
39 S. Pablo-García, S. Morandi, R. A. Vargas-Hernández, K. Jorner, Ž. Ivković, N. López and A. Aspuru-Guzik, *Nat. Comput. Sci.*, 2023, **3**, 433–442.

